Available online at www.scholarsresearchlibrary.com

Scholars Research Library

Der Pharmacia Lettre, 2014, 6 (6):20-34
(http://scholarsresearchlibrary.com/archive.html)

Scholars Research Library
ISSN 0975-5071
USA CODEN: DPLEB4

An electrochemical and theoretical evaluation of new quinoline derivative as a corrosion inhibitor for carbon steel in HCl solutions

H. Tayebi[1], H. Bourazmi[1], B. Himmi[4] A. El Assyry[5], Y. Ramli[3], A. Zarrouk[2], A. Geunbour[1], B. Hammouti[2] and Eno E. Ebenso[6]

[1]Laboratoire Corrosion-Électrochimie, Faculté des Sciences, Université Mohamed V, Rabat, Morocco
[2]LCAE-URAC18, Faculté des Sciences, Université Mohammed 1er, Oujda, Morocco
[3]Laboratoire de Chimie Thérapeutique, Faculté de Médecine et de Pharmacie de rabat, Université Mohamed V, Rabat, Morocco
[4]Filière Techniques de Santé, Institut des Professions Infirmières et des Techniques de Santé de Rabat, Morocco
[5]Laboratoire d'Optoélectronique et de Physico-chimie des Matériaux (Unité associée au CNRST), Département de Physique,Université Ibn Tofail, Kénitra, Maroc
[6]Material Science Innovation & Modelling (MaSIM) Research Focus Area, Faculty of Agriculture, Science and Technology, North-West University (Mafikeng Campus), Private Bag X2046, Mmabatho, South Africa

---

ABSTRACT

Inhibiting effect of 5-(chloromethyl)quinolin-8-ol Hydrochloride (QIN1) on carbon steel corrosion (CS) in 1.0 M HCl solution was investigated by electrochemical impedance spectroscopy and potentiodynamic measurements at 303-333 K in the presence of different concentrations of QIN1 ranging from 10^{-3}M to 10^{-6}M. Potentiodynamic polarization study clearly revealed that compound acted as mixed type inhibitor. Further, the quantum chemical calculations using density functional theory (DFT) gave a profound insight into the inhibition action mechanism of QIN1 and their calculation parameters such as E_{HOMO}, E_{LUMO} and ΔE are corroborative with the results of experimental studies. The various thermodynamic parameters of dissolution processes were evaluated in order to elaborate adsorption mechanism. Adsorption of inhibitor obeyed Langmuir adsorption isotherm model.

Keywords: Carbon steel, EIS, Polarisation, Quantum chemical calculations, Acid corrosion.

INTRODUCTION

Organic inhibitors were applied extensively to protect metals from corrosion in many aggressive acidic media (e.g. in the acid pickling and cleaning processes of metals) [1-3]. Organic compounds containing N, S and O atoms [4-24] were found to be good corrosion inhibitors of metals particularly for active metals. The effectiveness of theses compounds as corrosion inhibitors has been interpreted in terms of their molecular structure, molecular size, and molecular mass, hetero-atoms present and adsorptive tendencies [25]. Under certain conditions, the electronic structure of the organic inhibitors has a key influence on the corrosion inhibition efficiency to the metal. The inhibitors influence the kinetics of the electrochemical reactions which constitute the corrosion process and thereby modify the metal dissolution in acids. The existing data show that most organic inhibitors act by adsorption on the metal surface. They change the structure of the electrical double layer by adsorption on the metal surface. Quite a number of studies have been carried out in determination of adsorptivity of various compounds at the electrode/solution interface [26,27].

Thus the objective of the present work is to investigate the inhibition performance of the newly synthesised quinoline on carbon steel corrosion in hydrochloric acid. Ascertaining the corrosion inhibition on carbon steel was done at different concentrations of QIN1 by the electrochemical techniques such as, electrochemical impedance

spectroscopy and potentiodynamic polarization. Quantum chemical calculations were successively carried out to obtain the invaluable quantum chemical parameters such as E_{HOMO} and E_{LUMO} to understand the adsorption properties. The structure of QIN1 is shown in Figure 1.

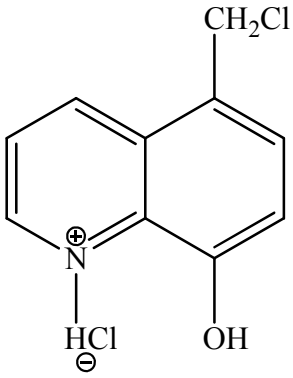

Figure 1. Structure of 5-(chloromethyl)quinolin-8-ol Hydrochloride (QIN1)

MATERIALS AND METHODS

Materials

The steel used in this study is a carbon steel (CS) (Euronorm: C35E carbon steel and US specification: SAE 1035) with a chemical composition (in wt%) of 0.370 % C, 0.230 % Si, 0.680 % Mn, 0.016 % S, 0.077 % Cr, 0.011 % Ti, 0.059 % Ni, 0.009 % Co, 0.160 % Cu and the remainder iron (Fe).

Solutions

The aggressive solutions of 1.0 M HCl were prepared by dilution of analytical grade 37% HCl with distilled water. The concentration range of Structure of 5-(chloromethyl)quinolin-8-ol Hydrochloride used was 10^{-6} M to 10^{-3} M.

Polarization measurements

Electrochemical impedance spectroscopy

The electrochemical measurements were carried out using Volta lab (Tacussel- Radiometer PGZ 100) potentiostate and controlled by Tacussel corrosion analysis software model (Voltamaster 4) at under static condition. The corrosion cell used had three electrodes. The reference electrode was a saturated calomel electrode (SCE). A platinum electrode was used as auxiliary electrode of surface area of 1 cm^2. The working electrode was carbon steel. All potentials given in this study were referred to this reference electrode. The working electrode was immersed in test solution for 30 minutes to a establish steady state open circuit potential (*E*ocp). After measuring the *E*ocp, the electrochemical measurements were performed. All electrochemical tests have been performed in aerated solutions at 303 K. The EIS experiments were conducted in the frequency range with high limit of 100 kHz and different low limit

0.1 Hz at open circuit potential, with 10 points per decade, at the rest potential, after 30 min of acid immersion, by applying 10 mV ac voltage peak-to-peak. Nyquist plots were made from these experiments. The best semicircle can be fit through the data points in the Nyquist plot using a non-linear least square fit so as to give the intersections with the *x*-axis.

The inhibition efficiency of the inhibitor was calculated from the charge transfer resistance values using the following equation [28]:

$$\eta_z\% = \frac{R_{ct}^{i} - R_{ct}^{\circ}}{R_{ct}^{i}} \times 100 \qquad (1)$$

where, R_{ct}° and R_{ct}^{i} are the charge transfer resistance in absence and in presence of inhibitor, respectively.

Potentiodynamic polarization

The electrochemical behaviour of carbon steel sample in inhibited and uninhibited solution was studied by recording anodic and cathodic potentiodynamic polarization curves. Measurements were performed in the 1.0 M HCl solution containing different concentrations of the tested inhibitor by changing the electrode potential automatically from -800 to 0 mV versus corrosion potential at a scan rate of 1 mV s^{-1}. The linear Tafel segments of anodic and cathodic

curves were extrapolated to corrosion potential to obtain corrosion current densities (I_{corr}). From the polarization curves obtained, the corrosion current (I_{corr}) was calculated by curve fitting using the equation:

$$I = I_{corr}\left[exp\left(\frac{2.3\Delta E}{\beta_a}\right) - exp\left(\frac{2.3\Delta E}{\beta_c}\right)\right] \quad (2)$$

β_a and β_c are the anodic and cathodic Tafel slopes and ΔE is $E\text{-}E_{corr}$.

The inhibition efficiency was evaluated from the measured I_{corr} values using the relationship:

$$\eta_{Tafel}\% = \frac{I^{\circ}_{corr} - I^{i}_{corr}}{I^{\circ}_{corr}} \times 100 \quad (3)$$

where, I°_{corr} and I^{i}_{corr} are the corrosion current density in absence and presence of inhibitor, respectively.

Computational procedures

Density Functional theory (DFT) has been recently used [29-32] to describe the interaction between the inhibitor molecule and the surface as well as the properties of these inhibitors concerning their reactivity. The molecular band gap was computed as the first vertical electronic excitation energy from the ground state using the time-dependent density functional theory (TD-DFT) approach as implemented in Gaussian 03 [33]. For these seek, some molecular descriptors, such as HOMO and LUMO energy values, frontier orbital energy gap, molecular dipole moment, electronegativity (χ), global hardness (η), softness(S), the fraction of electron transferred (ΔN), were calculated using the DFT method and have been used to understand the properties and activity of the newly prepared compounds and to help in the explanation of the experimental data obtained for the corrosion process.

According to Koopman's theorem [34] the ionization potential (IE) and electron affinity (EA) of the inhibitors are calculated using the following equations.

$IE = -E_{HOMO}$ (4)

$EA = -E_{LUMO}$ (5)

Thus, the values of the electronegativity (χ) and the chemical hardness (η) according to Pearson, operational and approximate definitions can be evaluated using the following relations [35]:

$$\chi = \frac{IE + EA}{2} \quad (6)$$

$$\eta = \frac{IE - EA}{2} \quad (7)$$

Global chemical softness (σ), which describes the capacity of an atom or group of atoms to receive electrons [36], was estimated by using the equation:

$$\sigma = \frac{1}{\eta} = -\frac{2}{E_{HOMO} - E_{LUMO}} \quad (8)$$

The number of transferred electrons (ΔN) was also calculated depending on the quantum chemical method [37,38] by using the equation:

$$\Delta N = \frac{\chi_{Fe} - \chi_{inh}}{2\left(\eta_{Fe} + \eta_{inh}\right)} \quad (9)$$

Where χ_{Fe} and χ_{inh} denote the absolute electronegativity of iron and inhibitor molecule η_{Fe} and η_{inh} denote the absolute hardness of iron and the inhibitor molecule respectively. In this study, we use the theoretical value of χ_{Fe} =7.0 eV and η_{Fe} = 0, for calculating the number of electron transferred.

RESULTS AND DISCUSSION

Potentiodynamic polarization

The potentiodynamic polarization curves for carbon steel in 1.0 M HCl solution in the absence and presence of different concentrations of this inhibitor, are shown in Fig. 2 at 303K. It is apparent from the Fig. 2, that the nature of the polarization curves remains the same in the absence and presence of inhibitor but the curves shifted towards lower current density in the presence of inhibitor, indicating that the inhibitor molecules retard the corrosion process. The corrosion current densities and corrosion potentials were calculated by extrapolation of the linear parts of anodic and cathodic curves to the point of intersection. The corrosion parameters such as corrosion potential (E_{corr}), cathodic Tafel slope (β_c), corrosion current density (I_{corr}) and percentage inhibition efficiency (η_{Tafel} %) obtained from these curves are given in Table 1.

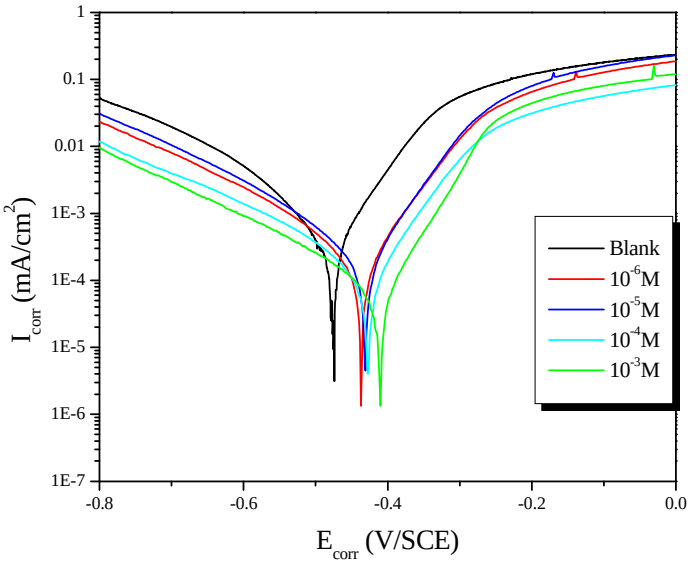

Figure 2. Typical polarization curves for carbon steel in 1.0 M HCl for various concentrations of QIN1 at 303 K

Table 1. Potentiodynamic electrochemical parameters for the corrosion of carbon steel in 1.0 M HCl solution in the absence and presence of the investigated inhibitor at 303 K

Inhibitor	Conc (M)	$-E_{corr}$ (mV_{SCE})	$-\beta_c$ (mV/dec)	I_{corr} ($\mu A\ cm^{-2}$)	η_{Tafel} (%)
Blank	1.0	476	124	335	-----
QIN1	10^{-3}	414	178	36	89
	10^{-4}	430	175	103	69
	10^{-5}	440	148	119	64
	10^{-6}	434	144	184	45

The results revealed that increasing the concentration of both inhibitors resulted in a decrease in corrosion current densities and an increase in inhibition efficiency (η_{Tafel} %), suggesting the adsorption of inhibitor molecules at the surface of carbon steel to form a protective film on the carbon steel surface [39]. The presence of an inhibitor causes a minor change in E_{corr} values with respect to the E_{corr} value in the absence of an inhibitor. This implies that the inhibitor act as a mixed-type inhibitor, affecting both anodic and cathodic reactions [40]. If the displacement in E_{corr} is more than ±85mV relating to the corrosion potential of the blank, the inhibitor can be considered as a cathodic or anodic type [41]. If the change in E_{corr} is less than ±85 mV, the corrosion inhibitor may be regarded as a mixed type. The maximum displacement in our study is 62 mV, which indicates that this inhibitor act as a mixed-type.

Electrochemical impedance spectroscopy studies

Effect of concentration

The Nyquist plots for carbon steel obtained at the interface in 1.0 M HCl solution with and without the different concentrations of QIN1 at 303K are shown in Fig. 3. The existence of a single semicircle with its center below in Nyquist plots (Fig. 3) for this inhibitor indicates the presence of a single charge transfer process during metal dissolution which is unaffected by the presence of inhibitor molecules. The Nyquist plots in the absence and presence of inhibitors are characterized by one capacitive loop. The capacitive loops are not perfect semicircles because of the non-homogeneity and roughness of the carbon steel surface [42].

The electrochemical impedance spectroscopy (EIS) spectra of all tests were analyzed using the equivalent circuit shown in Fig. 4, which is a parallel combination of the charge transfer resistance (R_{ct}) and the CPE, both in series with the solution resistance (R_s). This type of electrochemical equivalent circuit was reported previously to model the iron/acid interface [43]. CPE is introduced instead of a pure double layer capacitance to give a more accurate fit as the double layer at the interface does not behave as an ideal capacitor.

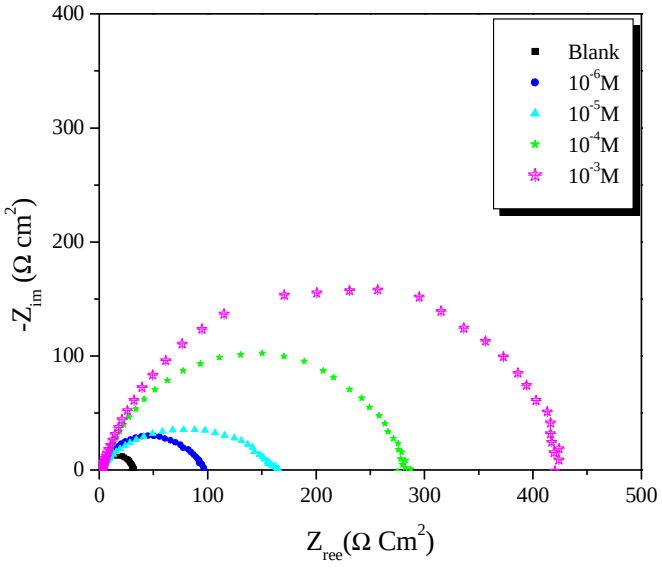

Figure 3. Nyqusit plots for carbon steel in 1.0 M HCl solution without and with different concentration of QIN1 at 303 K

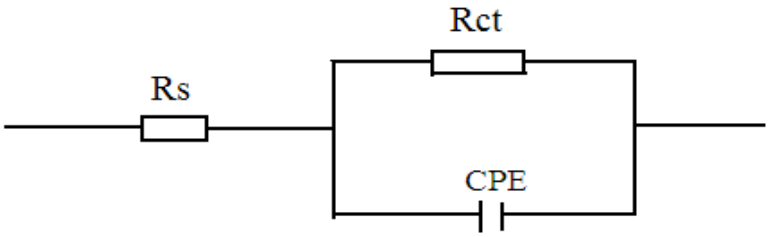

Figure 4. Equivalent circuit applied for fitting of the impedance spectra

The electrochemical parameters obtained from the fitting of the equivalent circuit are presented in Table 2. The data shown in Table 2 reveal that the value of R_{ct} increases with addition of inhibitor as compared to the blank solution; the increase in R_{ct} values is attributed to the formation of an insulating protective film at the metal/solution interface. The CPE value decreases on increasing the concentration of QIN1, indicating the adsorption of the inhibitor molecules on the surface of carbon steel. The single peak obtained in Bode plots (Fig. 5) for QIN1 indicates that the electrochemical impedance measurements fit well in a one-time constant equivalent model (Randle's cell model) with CPE.

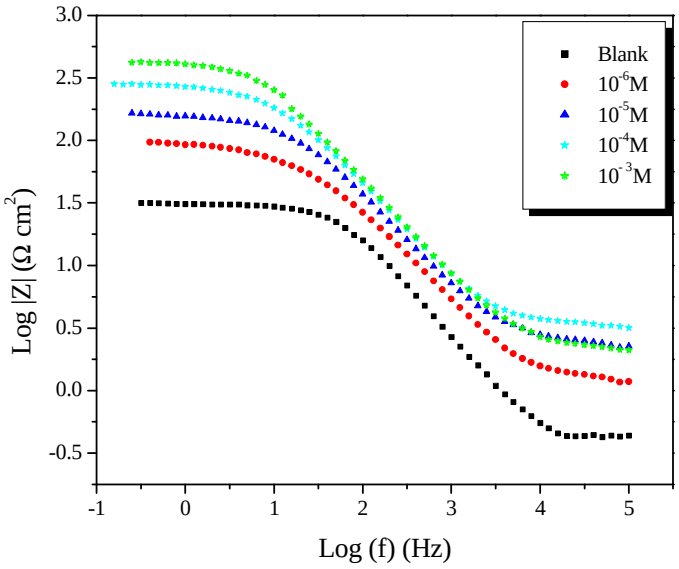

Figure 5. Bode plots for carbon steel in 1.0 M HCl solution without and with different concentration of QIN1 at 303 K

It is apparent that the impedance response for carbon steel in 1.0 M HCl changes significantly with increasing inhibitor concentration. Table 2 shows that the addition of the QIN1 into the corrosive solution caused to an increase in the inhibition efficiency, charge-transfer resistance and a decrease in the double-layer capacitance (C_{dl}) given as [14].

$$C_{dl} = \frac{\varepsilon \varepsilon_0 A}{d} \qquad (10)$$

where ε_0 is the vacuum dielectric constant, ε is the local dielectric constant, d is the thickness of the double layer, and A is the surface area of the electrode. According to Eq. 9, a decrease in C_{dl} can happen if the inhibitor molecules (low dielectric constant) replace the adsorbed water molecules (high dielectric constant) on the carbon steel surface. The capacitance is inversely proportional to the thickness of the double layer. Thus, decrease in the C_{dl} values could be attributed to the adsorption of QIN1 on the metal surface. Decrease in the capacitance, which can result from a decrease in the local dielectric constant and/or an increase in the thickness of the electrical double layer, strongly suggests that the inhibitor molecules adsorbed at the metal/solution interface. In the absence and in the presence of inhibitor, phase-shift value remains more or less identical; this indicates that the charge-transfer process controls the dissolution mechanism [44] of carbon steel in 1.0 M HCl solution. In acidic solutions, it is known that inhibitor molecules can be protonated. Thus, in solution, both neutral molecule and cationic forms of inhibitor exist [45]. It is assumed that Cl^- ion is first adsorbed onto the positively charged metal surface by coulombic attraction and then inhibitor molecules can be absorbed through electrostatic interactions between the positively charged molecules and the negatively charged metal surface [45]. These adsorbed molecules interact with ($FeCl^-$) adsspecies to form monomolecular layers (by forming a complex) on the steel surface. These layers protect carbon steel surface from attack by chloride ions. Thus, the oxidation of ($FeCl^-$) ads into Fe^{++} can be prevented. On the other hand, the protonated inhibitor molecules are also adsorbed at cathodic sites in competition with hydrogen ions that going to reduce hydrogen evolution. Inhibition performance of QIN1 for carbon steel/1.0 M HCl interface depends on several factors such as the number of adsorption sites, molecular size, mode of interaction with the metal surface, and extent of formation of metallic complexes [46].

Table 2. Electrochemical impedance parameters and inhibition efficiency for carbon steel in 1.0 M HCl solution with QIN1 at 303 K

	Conc (M)	R_{ct} (Ω cm^2)	f_{max} (Hz)	C_{dl} (μF/cm^2)	η_z (%)	θ
Blank	1.0	31	63.3	81	---	---
QIN1	10^{-3}	456	6.3	55	93	0.93
	10^{-4}	284	10	56	89	0.89
	10^{-5}	105	25	60	81	0.81
	10^{-6}	94	20	84	68	0.68

Effect of temperature

The effect of solution temperature on the impedance spectra recorded in the studied acid solutions without and with 1.0 mM of QIN1 has been studied. In all cases, the charge transfer resistances are decreased with increasing the temperature. Nyquist plots obtained at different temperatures in 1.0 M HCl solution without and with QIN1 are shown in Figs. 6 and 7, respectively. These spectra reveal that although values the charge transfer resistances are decreased with increasing the temperature, these values are higher in presence of QIN1 than in its absence. The impedance spectra obtained are quite similar to those obtained in 1.0 M HCl in the absence and presence of different concentrations of QIN1 at temperature.

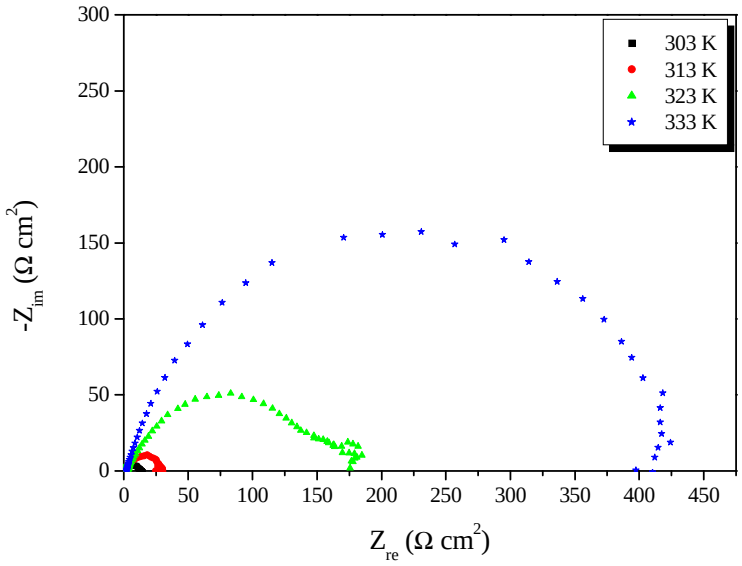

Figure 6. Nyquist diagrams for carbon steel in 1.0 M HCl at different temperatures

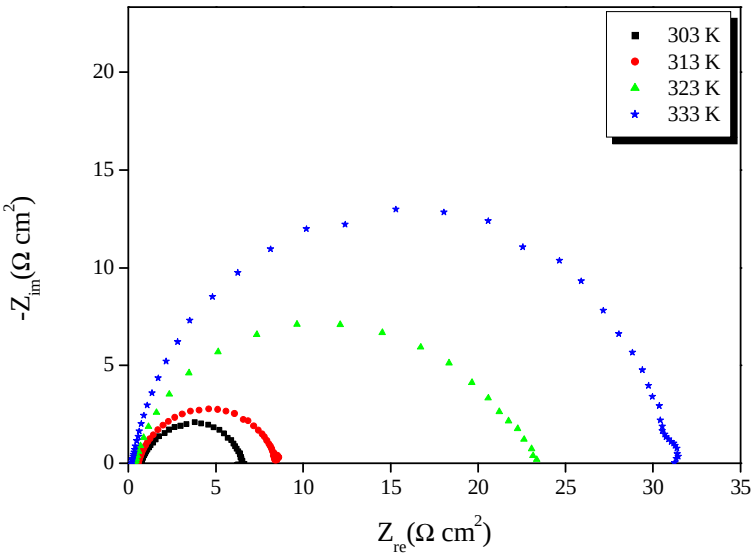

Figure 7. Nyquist diagrams for carbon steel in 1.0 M HCl + 1.0 mM of QIN1 at different temperatures

The various corrosion parameters obtained in 1.0 M HCl solution in absence and presence of 1.0 mM of QIN1 are given in Table 3. Values of R_{ct} obtained in presence and absence of quinoline derivative are decreased with increasing the temperature and its values are much higher in the inhibited acidic solutions which means the corrosion inhibition process by the QIN1. Values of C_{dl} obtained in 1.0 M HCl solution drastically increased indicating the high corrosion rate of steel at elevated temperatures and then remain approximately unchanged. In

presence of inhibitor, values of C_{dl} are slightly increased with the rise of temperature and are still lower than those obtained in the pure medium.

The influence of temperature on the inhibition efficiency of QIN1 in the investigated acid solution is shown in Table 3. The maximum η_z (93%) is obtained at 303 K. The decrease of η_z % of the QIN1 with increasing the temperature is a further evidence for the physical adsorption of the QIN1 on the electrode surface.

Table 3. Values of the elements of equivalent circuit required for fitting the EIS for carbon steel in 1.0 M HCl in the absence and presence of 1.0 mM of QIN1 at different temperatures

	Temp (K)	R_{ct} (Ω cm^2)	f_{max} (Hz)	C_{dl} (μF/cm^2)	η_z (%)
Blank	303	31	63.3	81	---
	313	27	40.1	147	---
	323	12	81.4	163	---
	333	6	158	168	---
QIN1	303	456	6.3	55	93
	313	180	13.6	65	85
	323	30	62.4	85	60
	333	13	90.7	135	54

Values of R_{ct} were employed to calculate values of the corrosion current density (I_{corr}) at various temperatures in absence and presence of QIN1 using the following equation [47]:

$$I_{corr} = RT\left(zFR_{ct}\right)^{-1} \quad (11)$$

where R is the universal gas constant (R = 8.314 J mol^{-1} K^{-1}), T is the absolute temperature, z is the valence of iron (z = 2), F is the Faraday constant (F = 96 485 coulomb) and R_{ct} is the charge transfer resistance.

Activation parameters such as the activation energy, E_a, the enthalpy of activation, ΔH_a, and the entropy of activation, ΔS_a, for both corrosion and corrosion inhibition of carbon steel in 1.0 M HCl in the absence and presence of 1.0 mM QIN1 between 303 and 333 K were calculated from an Arrhenius-type plot (Eq. (12)) and the transition state (Eq. (13)) [48,49]:

$$I_{corr} = k\exp\left(-\frac{E_a}{RT}\right) \quad (12)$$

where E_a is the apparent activation corrosion energy, T is the absolute temperature, k is the Arrhenius pre-exponential constant and R is the universal gas constant.

$$I_{corr} = \frac{RT}{Nh}\exp\left(\frac{\Delta S_a}{R}\right)\exp\left(-\frac{\Delta H_a}{RT}\right) \quad (13)$$

where h is Planck's constant, N is Avogadro's number, ΔS_a is the entropy of activation and ΔH_a is the enthalpy of activation.

Plots of Ln (I_{corr}) vs. 1000/T and Ln (I_{corr}/T) vs. 1000/T gave straight lines with slopes of $-E_a/R$ and $-\Delta H_a/R$, respectively. The intercepts were A and [Ln (R/Nh) + (ΔS_a/R)] for the Arrhenius and transition state equations, respectively. Figs. 8 and 9 represent the data plots of Ln (I_{corr}) vs. 1000/T and Ln (I_{corr}/T) vs. 1000/T in the absence and presence of 1.0 mM QIN1, representative example.

The calculated values from both methods of the activation energy, E_a, the enthalpy of activation, ΔH_a, and the entropy of activation, ΔS_a, are tabulated in Table 4. Inspection of Table 4 shows that values of both E_a, ΔH_a obtained in presence of QIN1 are higher than those obtained in the inhibitor-free solution. This observation further supports the proposed physical adsorption mechanism.

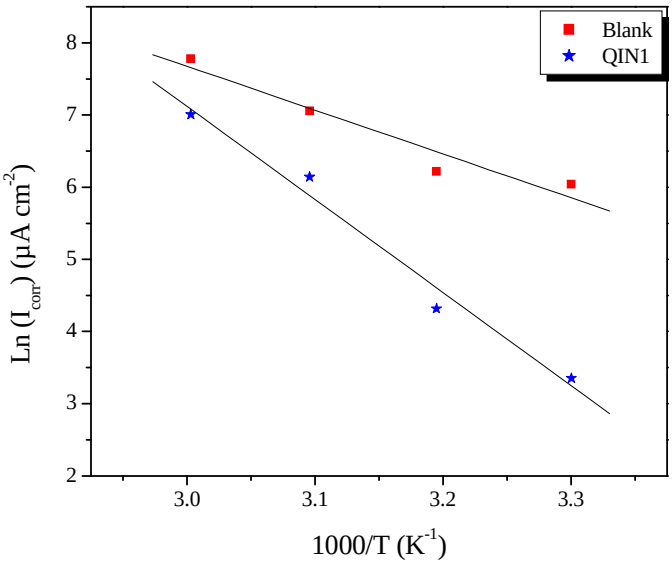

Figure 8. Arrhenius plots for carbon steel corrosion rates Ln (I_{corr}) versus 1/T in 1.0 M HCl in absence and in presence of 1.0 mM QIN3

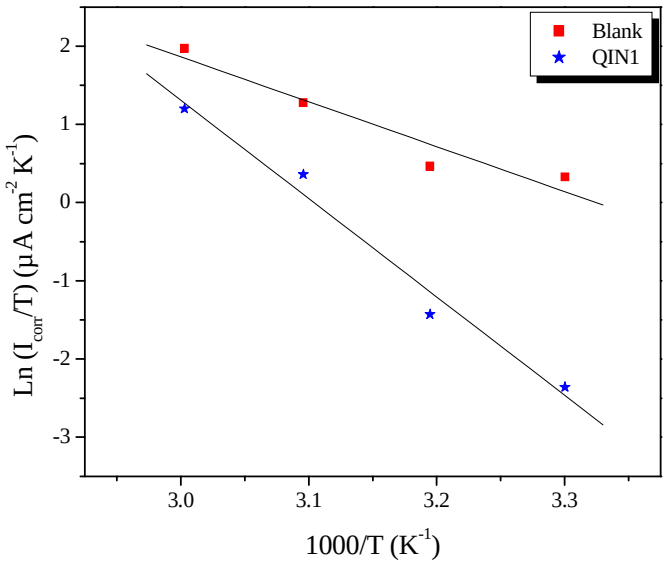

Figure 9. Transition-state plots for carbon steel corrosion rates Ln (I_{cor}r/T) versus 1/T in 1.0 M HCl in absence and in presence of 1.0 mM QIN3

Table 4. The value of activation parameters for carbon steel in 1.0 M HCl in the absence and presence of optimum concentration of QIN3

	E_a (kJ mol^{-1})	ΔH_a (kJ mol^{-1})	ΔS_a (J mol^{-1} K^{-1})
Blank	50.44	47.81	-38.61
QIN1	107.2	104.57	127.05

Higher values of E_a in inhibited systems compared to the blank have been reported [50-53] to be indicative of physical adsorption mechanism, while lower values of E_a suggest a chemisorption mechanism. On the other hand, the positive sign of ΔH_a reflects the endothermic nature of the carbon steel dissolution process suggesting that the dissolution of carbon steel is slow [54] in the presence of inhibitor. This behaviour can be explained as a result of the replacement process of water molecules during adsorption of QIN1 on steel surface [55,56]. The large negative value of ΔS_a for carbon steel in 1.0 M HCl implies that the activated complex is the rate-determining step, rather

than the dissociation step. In the presence of the inhibitor, the value of ΔS_a increases and is generally interpreted as an increase in disorder as the reactants are converted to the activated complexes [57].

Adsorption Isotherm

The values of surface coverage to different concentrations of inhibitors, obtained from impedance measurements at 303 K, have been used to explain the best isotherm to determine the adsorption process. Adsorption isotherms are very important in determining the mechanism of organo-electrochemical reactions [58]. The most frequently used isotherms are Langmiur, Temkin, Frumkin, Parsons, Hill de Boer, Flory-Huggins and Dahar-Flory-Huggins and Bockris-Swinkel [59-65]. All these isotherms are of the general form:

$$\int(\theta, x)\exp(2a\theta) = KC_{inh} \quad (14)$$

where $\int(\theta, x)$ is the configurational factor which depends upon the physical model and the assumptions underlying the derivation of the isotherm. "θ" is the surface coverage degree, "C_{inh}" is the inhibitor concentration in the bulk of solution "a" is the lateral interaction term describing the molecular interactions in the adsorption layer and the heterogeneity of the surface. "K" is the adsorption-desorption equilibrium constant. The surface coverage θ for different concentrations of QIN1 in 1.0 M HCl at 303 K has been evaluated from impedance spectroscopy.

Figs. 10, 11 and 12 represent fitting of impedance data obtained for carbon electrode in 1.0 M HCl containing various concentrations of QIN1 to Langmuir, Temkin and Frunkin isotherms (Eqs. 15, 16 and 17).

Langmuir isotherm: $$\frac{C_{inh}}{\theta} = \frac{1}{K} + C_{inh} \quad (15)$$

Frumkin isotherm: $$\left(\frac{\theta}{1-\theta}\right)\exp(-2a\theta) = KC_{inh} \quad (16)$$

Temkin isotherm: $$\exp(-2a\theta) = KC_{inh} \quad (17)$$

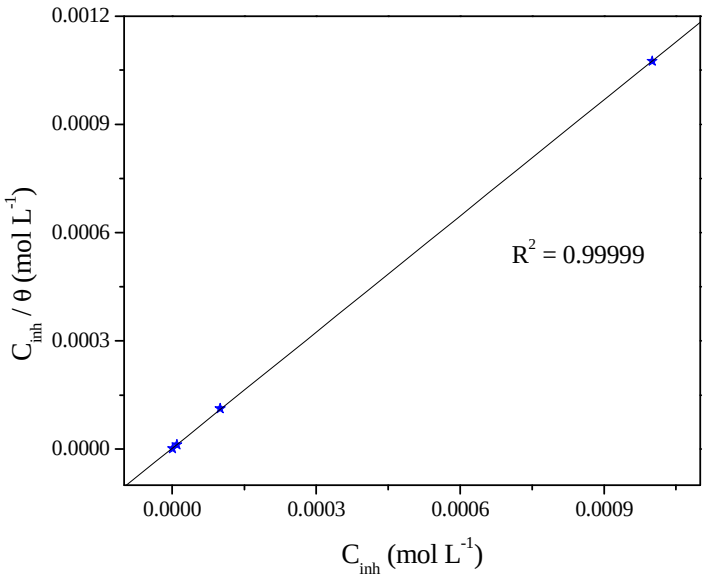

Figure 10. Langmuir adsorption plots for carbon steel in 1.0 M HCl containing different concentrations of QIN1

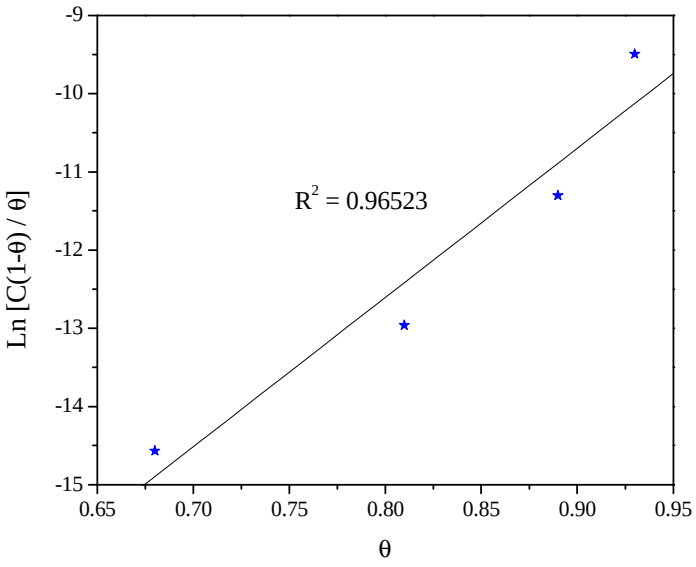

Figure 11. Frumkin adsorption plots for carbon steel in 1.0 M HCl containing different concentrations of QIN1

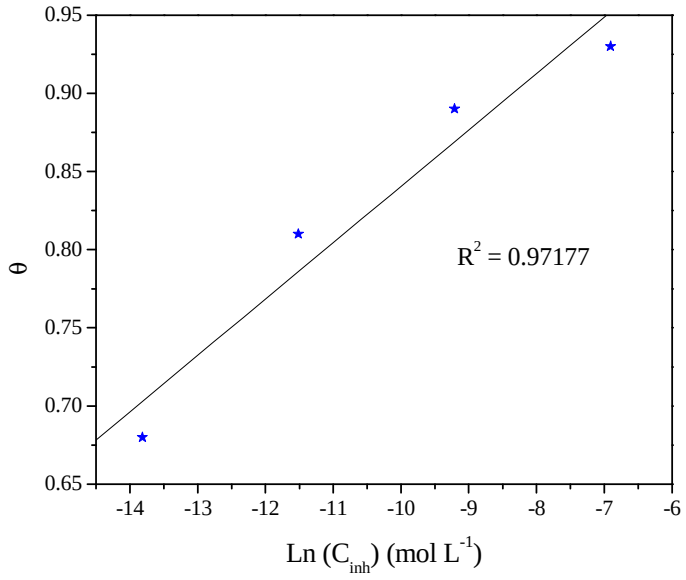

Figure 12. Temkin adsorption plots for carbon steel in 1.0 M HCl containing different concentrations of QIN1

The best correlation between the experimental results, obtained from the three tested isotherm functions was obtained using Langmuir adsorption isotherm. The values of correlation coefficient (R^2) were used to determine the best fit isotherm. Perfectly linear plots were obtained with correlation coefficient of 0.99999 using Langmuir adsorption isotherm.

The Langmuir isotherm is based on assumption that all adsorption sites are equivalent and that particle binding occurs independently from nearby sites being occupied or not [66]. It indicates that the adsorbing QIN1 species occupies typical adsorption site at the metal/solution interface. As can be seen by the good fit, QIN1 as inhibitor, found to follow Langmuir adsorption isotherm.

The equilibrium constant (K) for the adsorption-desorption process is related to the standard free energy of adsorption ΔG°_{ads}. The correlation between K and ΔG°_{ads} is shown in Eq. (18):

$$\Delta G^{\circ}_{ads} = -RTLn(55.5K) \quad (18)$$

Where R is the universal gas constant, T is the absolute temperature and the value of 55.5 is the concentration of water in the solution [67].

The thermodynamic parameters for the adsorption process obtained from Langmuir adsorption isotherm for the studied quinoline derivative is given in Table 5.

Table 3.Thermodynamic parameters for the adsorption of QIN1 in 1.0 M HCl on the carbon steel at 303 K

Inhibitor	Slope	R^2	K (M^{-1})	ΔG°_{ads} (KJ/mol)
QIN1	1.07	0.99999	442960.04	-42.87

It has been well understood that the standard free energy of adsorption values of -20 kJ mol^{-1} or less negative values are attributed to an electrostatic interaction between the charged molecules and the charged metal surface (physical adsorption) [68]. However, the standard free energy of adsorption values of -40 kJ mol^{-1} or more negative values show charge sharing or transfer from the inhibitor molecules to the metal surface to form a coordinate covalent bond [68]. Calculated ΔG°_{ads} value indicate that the adsorption mechanism of the synthesized quinoline derivative on carbon steel in 1.0 M HCl solution is chemical adsorption.

Theoretical studies

From the experimental results possible to get better performance of QIN1 as corrosion inhibitor. QIN1 ability to act as corrosion inhibitor were investigated by theoretical calculations. The high occupied molecular orbital, lowest unoccupied molecular orbital has been show in the Fig 13. The electronic properties such as energy of highest occupied molecular orbital (E_{HOMO}), energy of lowest unoccupied molecular orbital (E_{LUMO}), energy gap (ΔE) between LUMO and HOMO on the backbone atoms were determined by optimization. The optimized molecular structure is given in Fig.13 and electronic properties in Table 4. The HOMO and LUMO energies are correlated with percentage of inhibition efficiencies. The higher energy in HOMO orbital of inhibitor more eases to donate electrons unoccupied d orbital of the metallic iron. Lower energy in LUMO of inhibitor ease to accept electron form the metallic iron.

Lower energy in LUMO of inhibitor ease to accept electron form the metallic iron or aluminium. The inhibition efficiencies increase while QIN1 have higher HOMO energies, lower LUMO energies and decrease in energy gap between the HOMO and LUMO [69-72]. The values for E_{HOMO}, E_{LUMO} and ΔE in the table 4 shows that QIN1 have more ability to act as corrosion inhibitor. The HOMO density is great importance of mentioned transfer. Localization HOMO for QIN1 was distributed almost on the whole molecule, but the LUMO density is distributed at the ring quinoline and hydrochloric.

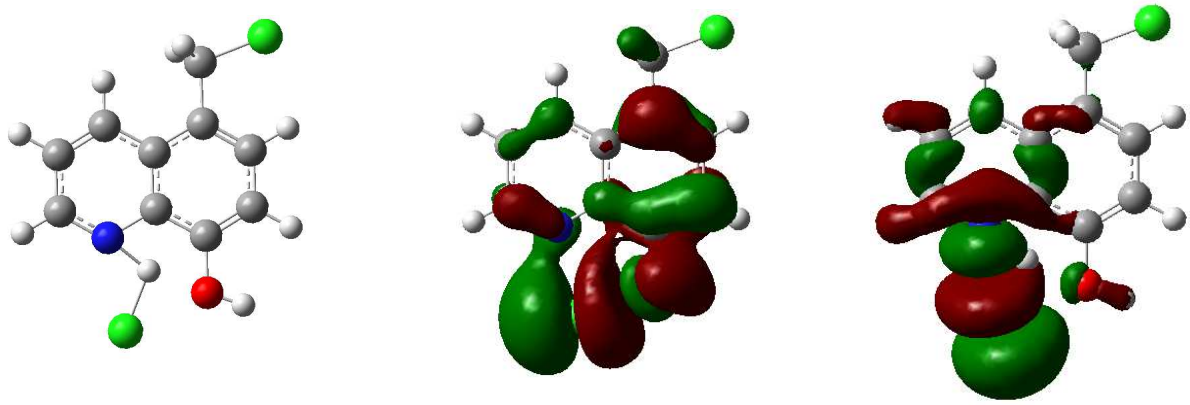

Figure 13. The optimized structure (left) and HOMO (center) and LUMO (right) distribution for QIN1

The quantum chemical parameters such as the energy of the highest occupied molecular orbital (E_{HOMO}), the energy of the lowest unoccupied molecular orbital (E_{LUMO}), energy gap ($\Delta E = E_{LUMO} - E_{HOMO}$), the dipole moment ($\mu$), Mulliken electronegativity (χ), global hardness (η), softness (σ), binding energy, molecular surface area and the fraction of electrons transferred (ΔN) were calculated and summarized in Table 4.

Table 4. Quantum chemical parameters for QIN1

	E_{HOMO} (eV)	E_{LUMO} (eV	ΔE (eV)	μ (D)	χ	σ	η	ΔN
QIN1	- 8.5171	- 8.2178	0.2993	3.0227	8.36755	0.14965		

Using Eq. 9, the value of electron-donating ability (ΔN) was calculated and its value is given in Table 6. If ΔN < 3.6 (electron), the inhibition efficiency increases with increasing value of ΔN, while it decreased if ΔN > 3.6 (electron) [38,73]. In present contribution, QIN1 is the donor of electrons, and the iron surface atom was the acceptor. The QIN1 was bound to the mild steel surface, and thus formed inhibition adsorption layer against corrosion at carbon steel/hydrochloric acid solution interface.

CONCLUSION

5-(chloromethyl)quinolin-8-ol Hydrochloride has a considerable inhibition effect on carbon steel corrosion in 1.0 M HCl solution. Inhibition efficiency of this compound increases with increasing concentrations due to the formation of a film on the steel surface. The polarization plots indicated that the compound inhibit both anodic metal dissolution and cathodic hydrogen evolution reaction and act as mixed type inhibitors. Impedance measurements indicate that with increasing inhibitor concentration, the transfert charge resistance (R_{ct}) increases, while the double layer capacitance (C_{dl}) decreases. The adsorption of this compound on the carbon steel surface obeys the Langmuir adsorption isotherm. The thermodynamic activation parameters were calculated and discussed. Inhibition efficiencies calculated using polarization, impedance and quantum chemical calculation were in good agreement.

REFERENCES

[1] G.E. Badr, *Corros. Sci*. **2009**, 51, 2529.
[2] Y. Ren, Y. Luo, K. Zhang, G. Zhu, X. Tan, *Corros. Sci*. **2008**, 50, 3147.
[3] K. S. Jacob, G. Parameswaran, *Corros. Sci.* **2010**, 52, 224.
[4] M. Prajila, J. Sam, J. Bincy, J. Abraham, *J. Mater. Environ. Sci*. **2012**, 3, 1045.
[5] U.J. Naik, V.A. Panchal, A.S. Patel, N.K. Shah, *J. Mater. Environ. Sci*. **2012**, 3, 935.
[6] A. Ghazoui, R. Saddik, N. Benchat, B. Hammouti, M. Guenbour, A. Zarrouk, M. Ramdani, *Der Pharm. Chem*. **2012**, 4, 352.
[7] A. Zarrouk, B. Hammouti, H. Zarrok, I. Warad, M. Bouachrine, *Der Pharm. Chem*. **2011**, 3, 263.
[8] A. H. Al Hamzi, H. Zarrok, A. Zarrouk, R. Salghi, B. Hammouti, S. S. Al-Deyab, M. Bouachrine, A. Amine, F. Guenoun, *Int. J. Electrochem. Sci*. **2013**, 8, 2586.
[9] D. Ben Hmamou, R. Salghi, A. Zarrouk, M. Messali, H. Zarrok, M. Errami, B. Hammouti, Lh. Bazzi, A. Chakir, *Der Pharm. Chem*. **2012**, 4, 1496.
[10] A. Ghazoui, N. Bencaht, S. S. Al-Deyab, A. Zarrouk, B. Hammouti, M. Ramdani, M. Guenbour, *Int. J. Electrochem. Sci*. **2013**, 8, 2272.
[11] A. Zarrouk, H. Zarrok, R. Salghi, N. Bouroumane, B. Hammouti, S. S. Al-Deyab, R. Touzani, *Int. J. Electrochem. Sci*. **2012**, 7, 10215.
[12] H. Bendaha A. Zarrouk, A. Aouniti, B. Hammouti, S. El Kadiri, R. Salghi, R. Touzani, *Phys. Chem. News*, **2012**, 64, 95.
[13] A. Zarrouk, B. Hammouti, H. Zarrok, M. Bouachrine, K.F. Khaled, S.S. Al-Deyab, *Int. J. Electrochem. Sci*. **2012**, 6, 89.
[14] A. Ghazoui, R. Saddik, N. Benchat, M. Guenbour, B. Hammouti, S.S. Al-Deyab, A. Zarrouk, *Int. J. Electrochem. Sci*. **2012**, 7, 7080.
[15] H. Zarrok, K. Al Mamari, A. Zarrouk, R. Salghi, B. Hammouti, S. S. Al-Deyab, E. M. Essassi, F. Bentiss, H. Oudda, *Int. J. Electrochem. Sci*. **2012**, 7, 10338.
[16] H. Zarrok, A. Zarrouk, R. Salghi, Y. Ramli, B. Hammouti, M. Assouag, E. M. Essassi, H. Oudda, M. Taleb, *J. Chem. Pharm. Res*. **2012**, 4, 5048.
[17] H. Zarrok, A. Zarrouk, R. Salghi, H. Oudda, B. Hammouti, M. Assouag, M. Taleb, M. Ebn Touhami, M. Bouachrine, S. Boukhris, *J. Chem. Pharm. Res*. **2012**, 4, 5056.
[18] H. Zarrok, H. Oudda, A. El Midaoui, A. Zarrouk, B. Hammouti, M. Ebn Touhami, A. Attayibat, S. Radi, R. Touzani, *Res. Chem. Intermed*. **2012**, 38, 2051.
[19] A. Zarrouk, H. Zarrok, R. Salghi, B. Hammouti, F. Bentiss, R. Touir, M. Bouachrine, *J. Mater. Environ. Sci.* **2013**, 4, 177.
[20] A. Ghazoui, A. Zarrouk, N. Bencaht, R. Salghi, M. Assouag, M. El Hezzat, A. Guenbour, B. Hammouti, *J. Chem. Pharm. Res*. **2014**, 6, 704.
[21] H. Zarrok, A. Zarrouk, R. Salghi, M. Ebn Touhami, H. Oudda, B. Hammouti, R. Touir, F. Bentiss, S. S. Al-Deyab, *Int. J. Electrochem. Sci*. **2013**, 8, 6014.

[22] A. Zarrouk, H. Zarrok, R. Salghi, R. Touir, B. Hammouti, N. Benchat, L. Afrine, H. Hannache, M. El Hezzat, M. Bouachrine, *J. Chem. Pharm. Res*. **2013**, 5, 1482.
[23] D. Ben Hmamou, M. R. Aouad, R. Salghi, A. Zarrouk, M. Assouag, O. Benali, M. Messali, H. Zarrok, B. Hammouti, *J. Chem. Pharm. Res*. **2012**, 4, 3489.
[24] L. Afrine, A. Zarrouk, H. Zarrok, R. Salghi, R. Touir, B. Hammouti, H. Oudda, M. Assouag, H. Hannache, M. El Harti, M. Bouachrine, *J. Chem. Pharm. Res*. **2013**, 5, 1474.
[25] J. Aljourani, K. Raeissi, M. A. Golozar, *Corros. Sci*. **2009**, 51, 1836.
[26] M. Lebrini, M. Traisnel, M. Lagrenee, B. Mernari, F. Bentiss, *Corros. Sci*. **2008**, 50, 473.
[27] B. B. Damaskin, A. N. Frumkin, N.S. Hush (Ed.) Adsorption of molecules on electrodes, Wiley-Interscience, London, **1971**, p. 1.
[28] S. Rekkab, H. Zarrok, R. Salghi, A. Zarrouk, Lh. Bazzi, B. Hammouti, Z. Kabouche, R. Touzani , M. Zougagh, *J. Mater. Environ. Sci*. **2012**, 3, 613.
[29] H. Ma, S. Chen, Z. Liu,Y. Sun, *J. Mol. Struct., (THEOCHEM)* **2006**, 774, 1922.
[30] J.H. Henrquez-Romn, L. Padilla-Campos, M.A. Pez, J.H. Zagal, M.A.Rubio, C.M. Rangel, J. Costamagna, G. Crdenas-Jirn, *J. Mol. Struct., (THEOCHEM)* **2005**, 757, 17.
[31] L.M. Rodrguez-Valdez, A. Martnez-Villafane, D. Glossman-Mitnik, *J. Mol. Struct. (THEOCHEM)* **2005**, 713, 6570.
[32] Y. Feng, S. Chen, W. Guo, Y. Zhang, G. Liu, *J. Electroanal. Chem*. **2007**, 602, 115.
[33] M. J. Frisch, G. W. Trucks, H. B. Schlegel, G. E. Scuseria, M. A. Robb, J. R. Cheeseman, J. A. Montgomery, Jr., T. Vreven, K. N. Kudin, J. C. Burant, J. M. Millam, S. S. Iyengar, J. Tomasi, V. Barone, B. Mennucci, M. Cossi, G. Scalmani, N. Rega, G. A. Petersson, H. Nakatsuji, M. Hada, M. Ehara, K. Toyota, R. Fukuda, J. Hasegawa, M. Ishida, T. Nakajima, Y. Honda, O. Kitao, H. Nakai, M. Klene, X. Li, J. E. Knox, H. P. Hratchian, J. B. Cross, V. Bakken, C. Adamo, J. Jaramillo, R. Gomperts, R. E. Stratmann, O. Yazyev, A. J. Austin, R. Cammi, C. Pomelli, J. W. Ochterski, P. Y. Ayala, K. Morokuma, G. A. Voth, P. Salvador, J. J. Dannenberg, V. G. Zakrzewski, S. Dapprich, A. D. Daniels, M. C. Strain, O. Farkas, D. K. Malick, A. D. Rabuck, K. Raghavachari, J. B. Foresman, J. V. Ortiz, Q. Cui, A. G. Baboul, S. Clifford, J. Cioslowski, B. B. Stefanov, G. Liu, A. Liashenko, P. Piskorz, I. Komaromi, R. L. Martin, D. J. Fox, T. Keith, M. A. Al-Laham, C. Y. Peng, A. Nanayakkara, M. Challacombe, P. M. W. Gill, B. Johnson, W. Chen, M. W. Wong, C. Gonzalez, and J. A. Pople, *Gaussian 03, Revision E.01, Gaussian, Inc., Wallingford CT*, **2004**.
[34] M.J.S. Dewar, W. Thiel, *J. Am. Chem. Soc*. **1977**, 99, 4899.
[35] R.G. Pearson, *Inorg. Chem*. **1988**, 27, 734.
[36] J.H. Henríquez-Román, L. Padilla-Campos, M.A. Páez, J.H. Zagal, A. María Rubio, C.M. Rangel, J. Costamagna, G. Cárdenas-Jirón. *J. Mol. Struct., (THEOCHEM)* **2005**, 757, 1.
[37] V.S. Sastri, J.R. Perumareddi, *Corrosion (NACE)* **1997**, 53, 617.
[38] I. Lukovits, E. Kalman, F. Zucchi, *Corrosion (NACE)* **2001**, 57, 3.
[39] X. Wang, H. Yang, F. Wang, *Corros. Sci*. **2011**, 53, 113.
[40] D. Jayaperumal, *Mater. Chem. Phys*. **2010**, 119, 478.
[41] E. S. Ferreira, C. Giancomlli, F. C. Giacomlli, A. Spinelli, *Mater. Chem. Phys*. **2004**, 83, 129.
[42] S. Ramesh, S. Rajeswari, *Electrochim. Acta* **2004**, 49, 811.
[43] H. Ashassi-Sorkhabi, B. Shaabani, D. Seifzadeh, *App. Surf. Sci*. **2005**, 239, 154.
[44] A.A. Hermas, M.S. Morad, M.H. Wahdan *J. Appl. Electrochem*., **2004**, 34, 95.
[45] M.A. Quraishi, M.Z.A. Rafiquee, S. Khan, N. Saxena, *J. Appl. Electrochem*., **2007**, 37, 1153.
[46] F. Bentiss, M. Bouanis, B. Mernari, M. Traisnel, H. Vezin, M. Lagrenee, *Appl. Surf. Sci*., **2007**, 253, 3696.
[47] F. Beck, U.A. Kruger, *Electrochim. Acta*, **1996**, 41, 1083.
[48] S. Martinez, I. Stern, *Appl. Surf. Sci*. **2008**, 199, 83.
[49] P. Li, J.Y. Lin, K.L. Tan, J.Y. Lee, *Electrochim. Acta*, **1997**, 42, 605.
[50] G. Moretti, G. Quartaronr, A. Tassan, A. Zingales, *Electrochim. Acta*, **1996**, 41, 1971.
[51] B.M. Praveen, T.V. Venkatesha, *Int. J. Electrochem. Sci.* **2009**, 4, 267.
[52] M. Lebrini, F. Robert, C. Roos, *Int. J. Electrochem. Sci.* **2010**, 5, 1698.
[53] M. Lebrini, F. Robert, C. Roos, *Int. J. Electrochem. Sci.* **2011**, 6, 847.
[54] N.M. Guan, L. Xueming, L. Fei, *Mater. Chem. Phys.* **2004**, 86, 59.
[55] M.S. Abdel-Aal, M.S. Morad, Br. Corros. J. **2001**, 36, 253.
[56] O.K. Abialo, N.C. Oforka, *Mater. Chem. Phys.* **2004**, 83, 315.
[57] S.M.A. Hosseini, M. Salari, M. Ghasemi, M. Abaszadeh, *Z. Phys. Chem*., **2009**, 223, 769.
[58] X. Wu, H. Ma, S. Chen, Z. Xu, A. Sui, *J. Electrochem. Soc.* **1999**, 146, 1847.
[59] I. Langmuir, *J. Am. Chem. Soc.* **1917**, 39, 1848.
[60] R. Alberty, R. Silbey, Physical Chemistry, second ed., Wiley, New York, **1997**. p. 845.
[61] J.O'M. Bockris, S.U.M. Khan, Surface Electrochemistry: A Molecular Level Approach, Plenum Press, New York, **1993**.
[62] J.W. Schapinik, M. Oudeman, K.W. Leu, J.N. Helle, *Trans. Farad. Soc.* **1960**, 56, 415.

[63] O. Ikeda, H. Jimbo, H. Tamura, *J. Electroanal. Chem.* **1982**, 137, 127.
[64] J. Hill de Boer, The Dynamical Character of Adsorption, second ed., Clarendon Press, Oxford, UK, **1986**.
[65] H. Dhar, B. Conway, K. Joshi, *Electrochim. Acta*, **1973**, 18, 789.
[66] K.F. Khaled, N. Hackerman, *Electrochim. Acta*, **2003**, 48, 2715.
[67] O. Olivares, N.V. Likhanova, B. Gomez, J. Navarrete, M.E. Llanos-Serrano, E. Arce, J.M. Hallen, *Appl. Surf. Sci*., **2006**, 252, 2894.
[68] S.V. Ramesh, A.V. Adhikari, *Mater. Chem. Phys*., **2009**, 115, 618.
[69] S. John, A. Joseph, *RSC Adv.*, **2012**, 2, 9944.
[70] S. Safak, B. Duran, A. Yurt, G. Turkoglu, *Corros. Sci.*, **2012**, 54, 251.
[71] A.O. Yuce, G. Kardas, *Corros. Sci.*, **2012**, 58, 86.
[72] C.M. Goulart , A. Esteves-Souza, C.A. Martinez-Huitle, C.J.F. Rodrigues, M.A.M. Maciel, A. Echevarria, *Corros. Sci.*, **2013**, 67, 281.
[73] F. Bentiss, M. Traisnel, *J. Appl. Electrochem.*, **2001**, 31, 41.